Electronic Supplementary Material (ESI) for Journal of Materials Chemistry A.

Ultrasmall Fe_3O_4 Nanodots within N-Doped Carbon Frameworks from MOFs Uniformly Anchored on Carbon Nanowebs for Boosting Li-ion Storage

Yan Wang,[a,d] Youjun Gao,[b] Jie Shao,*[a,c] Rudolf Holze,*[c] Zheng Chen,[b] Yuanxing Yun,[d] Qunting Qu,*[d] Honghe Zheng[d]

[a] College of Chemistry, Chemical Engineering and Material Science, Soochow University, Suzhou, Jiangsu 215006, PR China

[b] College of Materials and Environmental Engineering, Hezhou University, Hezhou, Guangxi 542899, PR China

[c] Institut für Chemie, AG Elektrochemie, Technische Universität Chemnitz, 09111 Chemnitz, Germany

[d] College of Physics, Optoelectronics and Energy & Collaborative Innovation Center of Suzhou Nano Science and Technology, Soochow University, Suzhou, Jiangsu 215006, PR China

*E-mail: shaojie@suda.edu.cn; qtqu@suda.edu.cn; rudolf.holze@chemie.tu-chemnitz.de

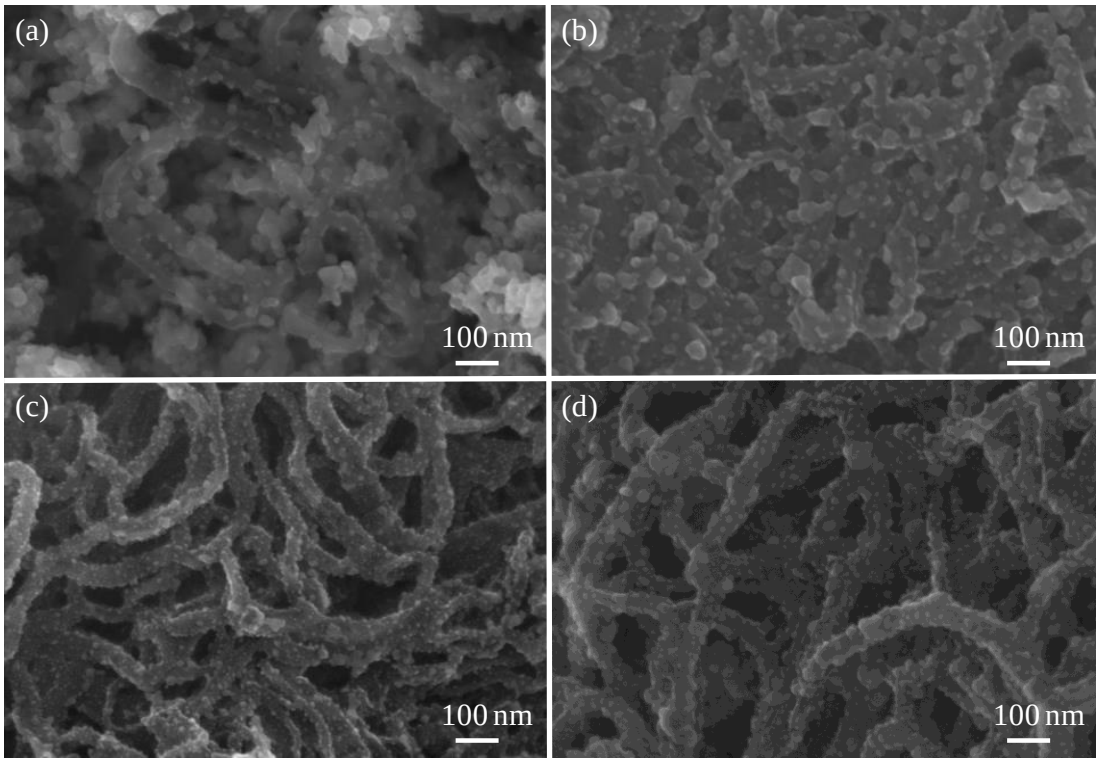

Figure S1 SEM images of NCW@Fe-ZIFs after reaction for (a) 30 min, (b) 1 h, (c) 3 h and (d) 5 h.

A very short reaction time (e.g., 30 min or 1 h) results in few Fe-ZIFs nanoparticles formed on NCW due to insufficient growth; whereas the excessive reaction time (e.g., 5 h) induces severe homogeneous growth of Fe-ZIFs particles.

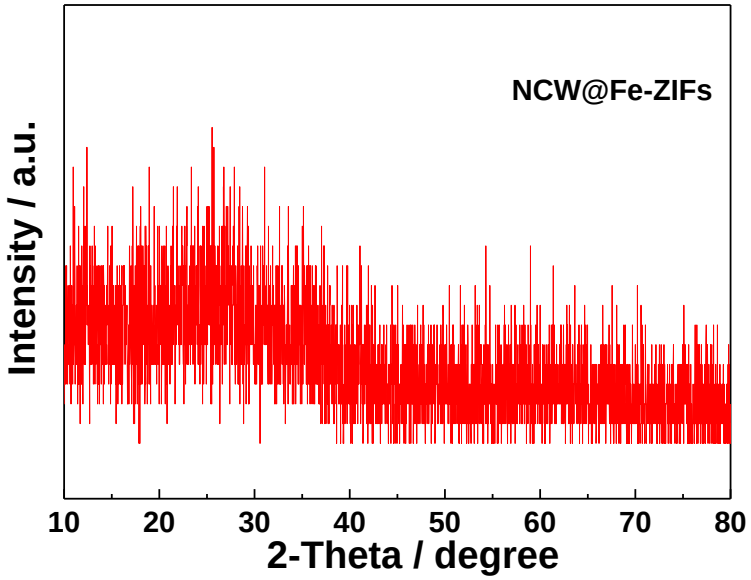

Figure S2 XRD pattern of NCW@Fe-ZIFs.

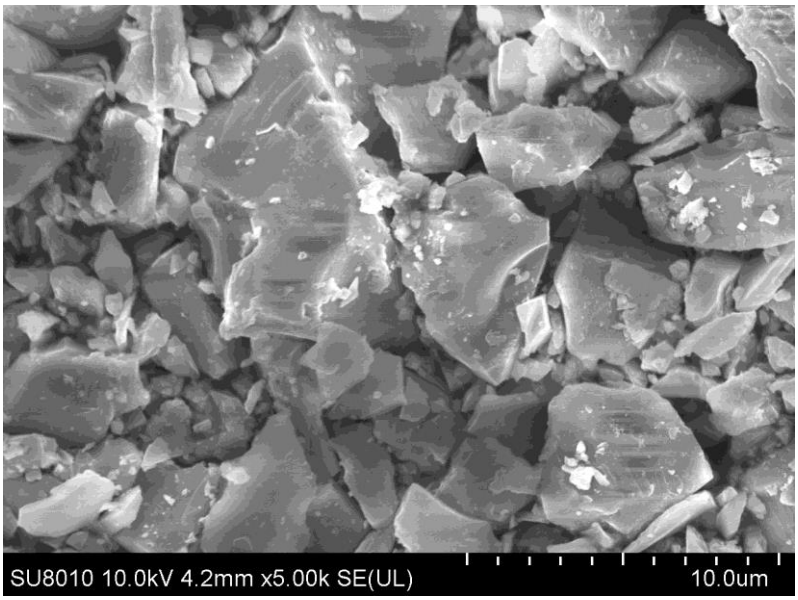

Figure S3 SEM image of pure Fe-ZIFs prepared through the same procedure described in this work except in the absence of NCW.

It can be seen that the morphology of pure Fe-ZIFs is irregular.

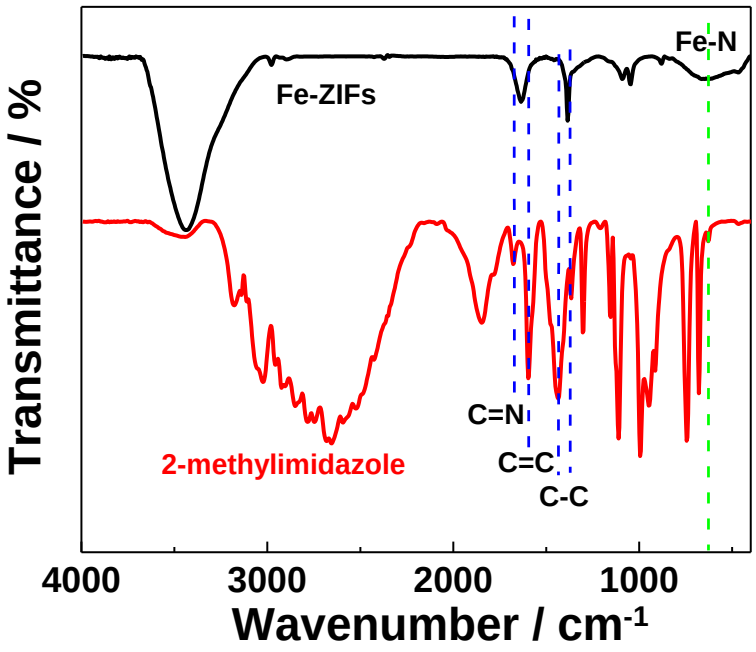

Figure S4 FTIR spectra of 2-methylimidazole and the as-prepared Fe-ZIFs.

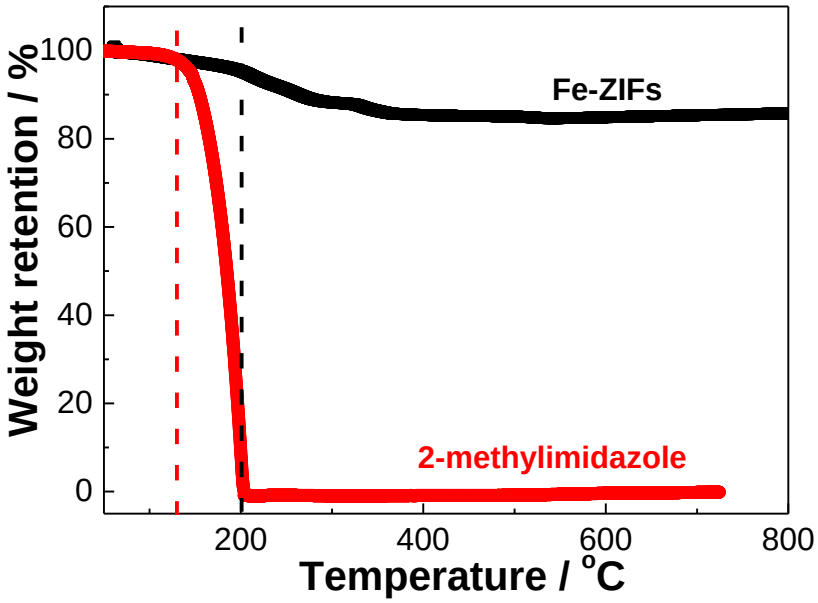

Figure S5 TG curves of 2-methylimidazole and the as-prepared Fe-ZIFs.

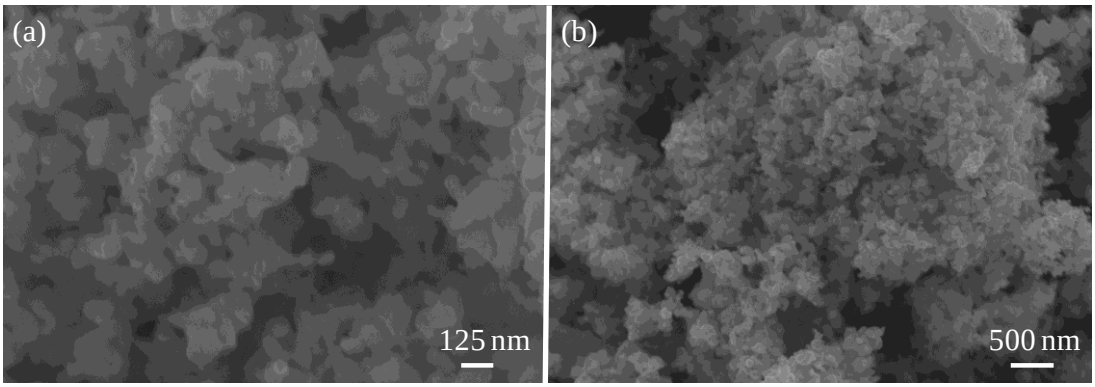

Figure S6 (a and b) SEM images of Fe_3O_4/NC composite prepared in the absence of NCW.

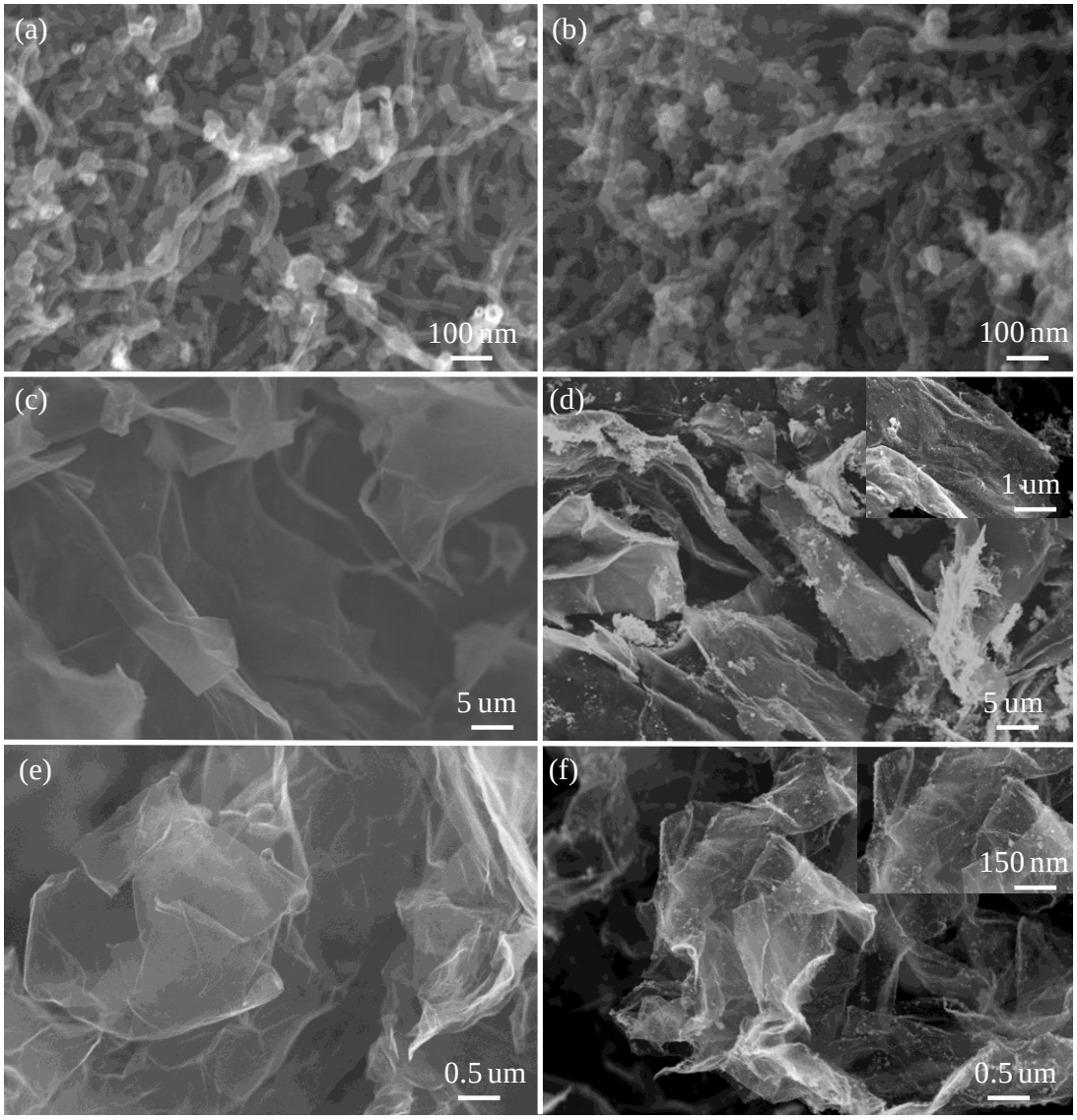

Figure S7 SEM images of (a) CNT, (b) CNT@Fe-ZIFs, (c) GO, (d) GO@Fe-ZIFs, (e) graphene, and (f) graphene@Fe-ZIFs.

CNT@Fe-ZIFs, GO@Fe-ZIFs and graphene@Fe-ZIFs were prepared through the similar approach with NCW@Fe-ZIFs except that CNT, graphene oxide (GO) and grapheme were used as the carbon substrates, respectively. The uniform distribution of Fe-ZIFs on carbon substrates is clearly observed, demonstrating the wide applicability of this strategy.

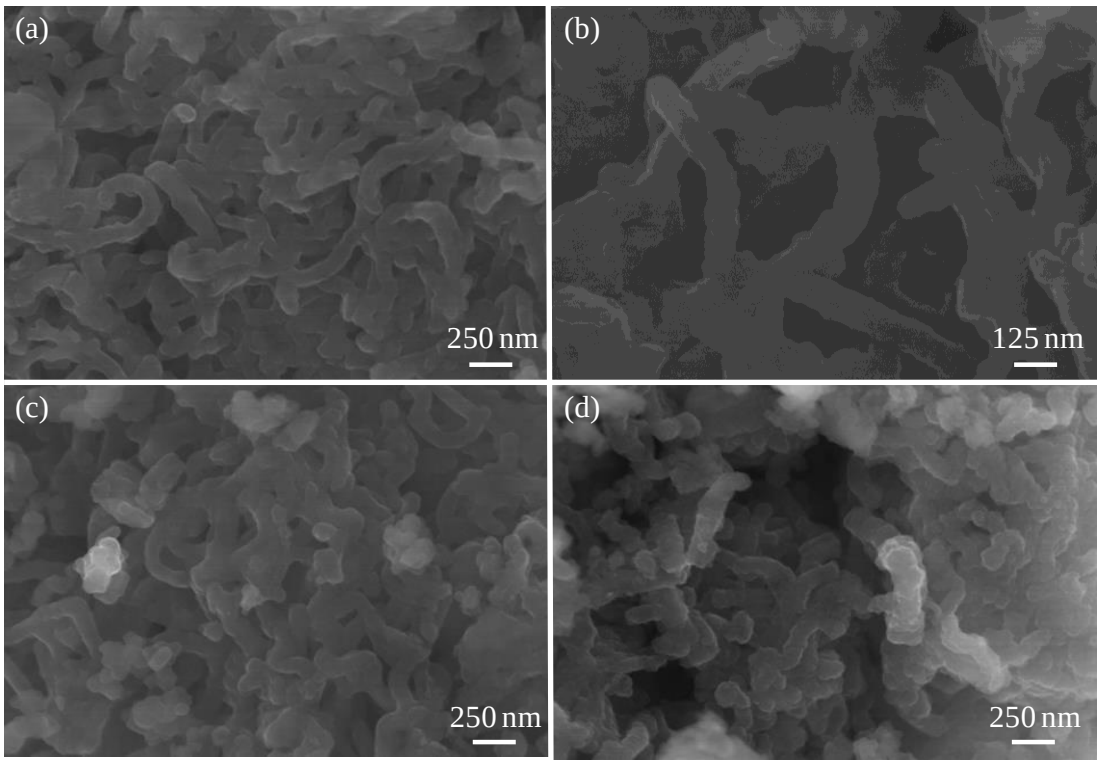

Figure S8 SEM images of NCW@Co-ZIFs after reaction for (a and b) 30 min, (c) 60 min and (d) 120 min.

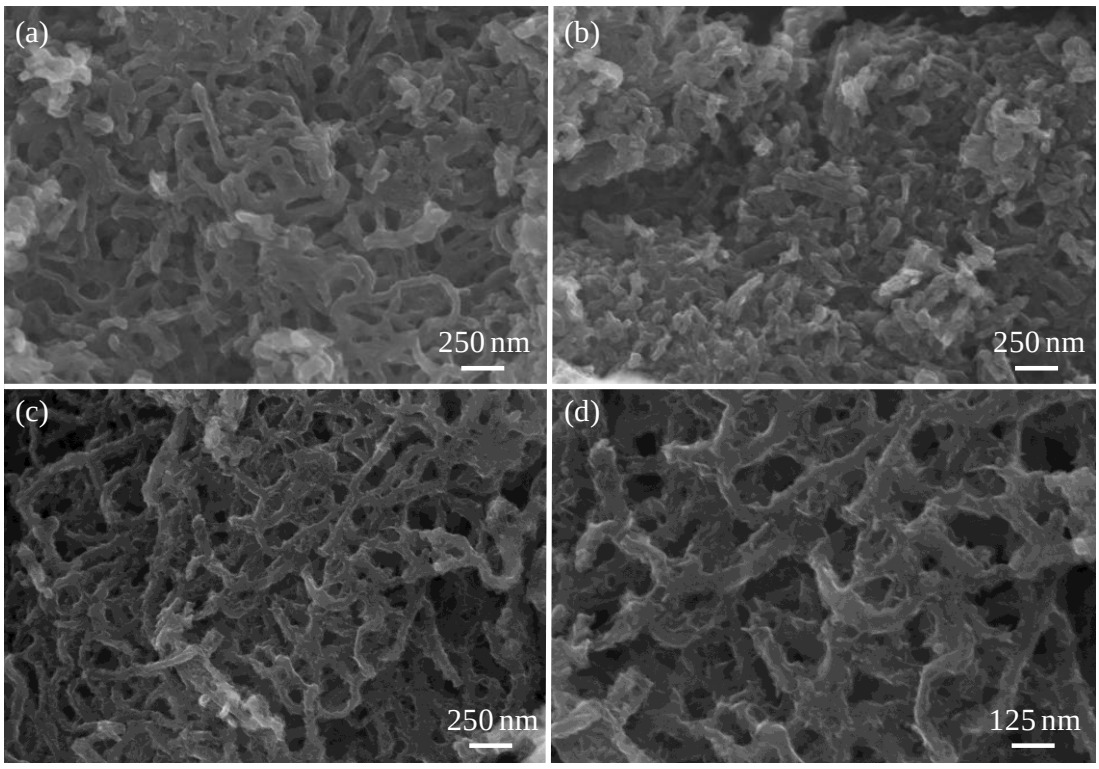

Figure S9 SEM images of NCW@Ni-ZIFs after reaction for (a) 2 h, (c and d) 4 h, and (b) 6 h.

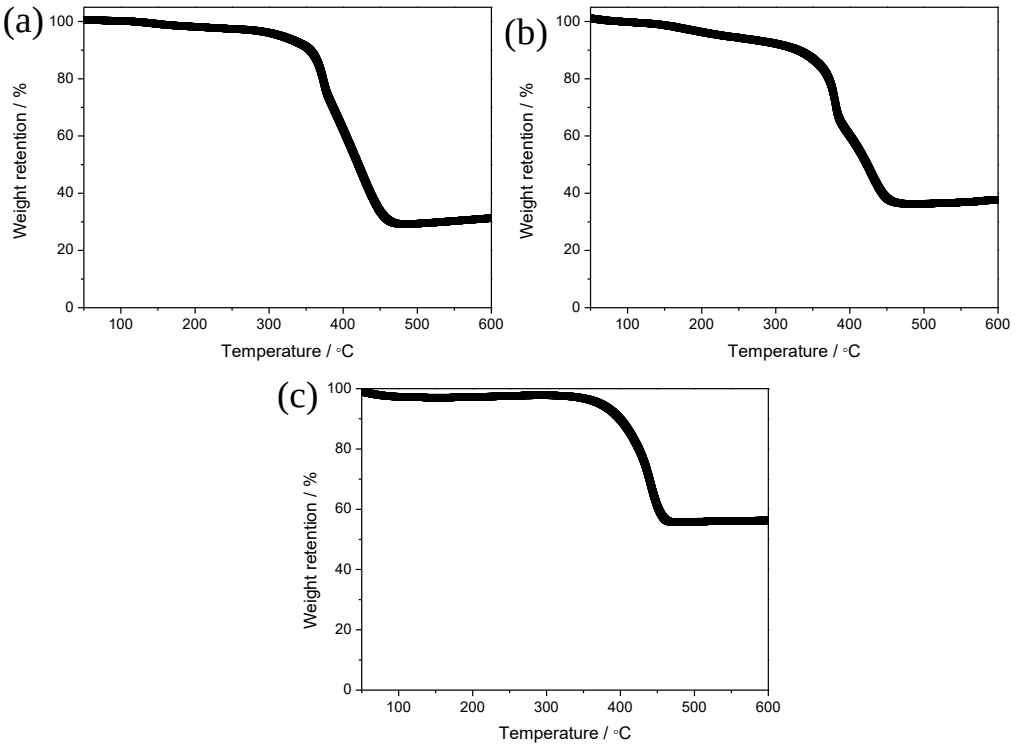

Figure S10 TG curves of pyrolyzed products derived from (a) NCW@Ni-ZIFs, (b) NCW@Co-ZIFs and (c) NCW@Fe-ZIFs under air flow.

In order to accurately compare the contents of active substances in different MOFs-derived materials, NCW@Ni-ZIFs and NCW@Co-ZIFs were calcined under the same conditions (Ar, 500 ^{o}C, 3h) with NCW@Fe-ZIFs.

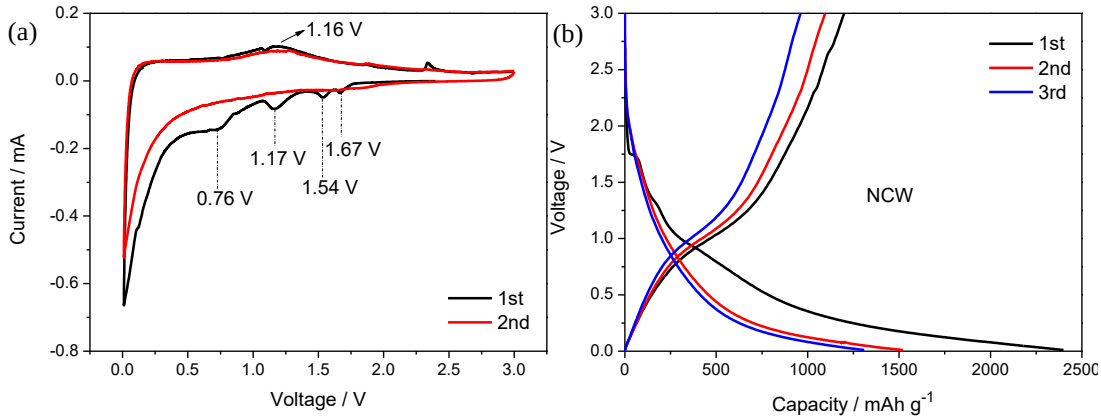

Figure S11 (a) CV curves and (b) the initial three galvanostatic discharge/charge curves of NCW electrode.

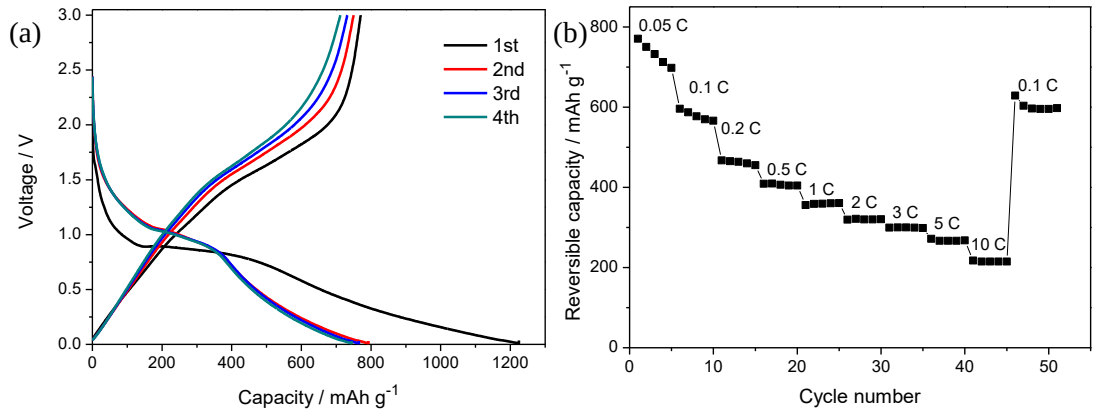

Figure S12 (a) The initial four galvanostatic discharge/charge curves and (b) rate capability of Fe_3O_4/NC electrodes at various current densities.

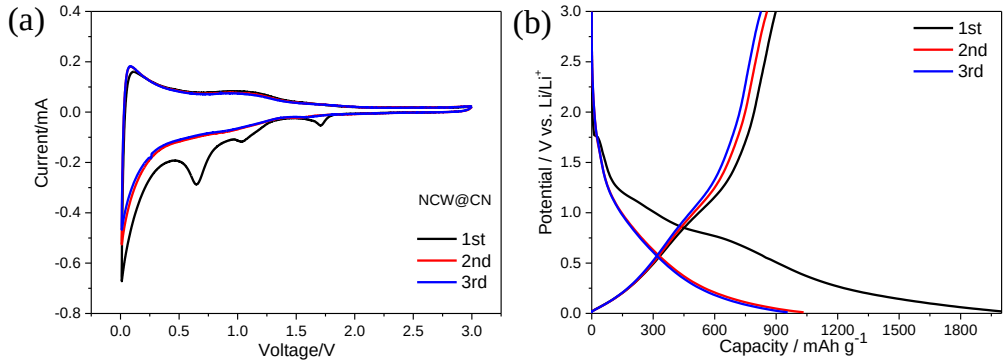

Figure S13 (a) CV curves and (b) the initial three galvanostatic discharge/charge curves of NCW@NC electrode.

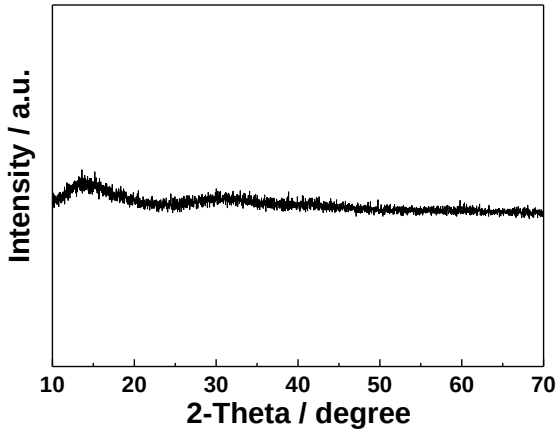

Figure S14 XRD pattern of the NCW@Fe_3O_4/NC electrode after 200 discharge/charge cycles.

As shown in Figure S14, no obvious diffraction peaks are observed, so it is believed that amorphization of Fe_3O_4 nanodots may occur after the long-term cycling.